Structures 5 (2016) 161–169

Contents lists available at ScienceDirect

Structures

journal homepage: www.elsevier.com/locate/structures

Application of Intelligent Passive Devices Based on Shape Memory Alloys in Seismic Control of Structures

Behrouz Asgarian, Neda Salari *, Behnam Saadati

Civil Engineering Faculty, K.N. Toosi University of Technology, Tehran, Iran

ARTICLE INFO

Article history:
Received 5 May 2015
Received in revised form 27 September 2015
Accepted 31 October 2015
Available online 10 November 2015

Keywords:
Shape Memory Alloy
Self-centering hybrid damper
Nonlinear time-history analysis
Roof permanent displacement
Roof acceleration

ABSTRACT

In this study, seismic application of an innovative control device called self-centering hybrid damper (SCHD) is investigated. Two main characteristics of the SCHD result in structural response mitigation. Steel pipe as a vertical link and two transverse pairs of Shape Memory Alloy (SMA) wires are used as energy dissipation and recentering components, respectively. Adjustable design parameters including design load, incorporation percentage of SMA, pipe height and wire inclination angle provide desirable structural responses. A numerical parametric study revealed the effect of each parameter on device performance. Besides, an optimum incorporation percentage of SMA in design load was obtained from the parametric study. The results also indicated that in addition to ideal energy dissipation capability, SCHDs can effectively reduce the permanent displacement. Nonlinear time-history analysis of a 5-story building equipped with the SCHD was conducted to evaluate the effectiveness of the device. The results indicated that utilization of the proposed innovative damper is an effective way in reduction of roof acceleration, peak interstory drift and permanent displacement.

1. Introduction

In recent years, various design philosophies have been developed to reduce the economical losses and inelastic deformations of structures under strong ground motions. After the 1994 Northridge earthquake, supplemental energy dissipation devices have been introduced to improve the resistance of structures. A wide range of materials can be used in passive energy dissipation systems to improve the structural responses [1, 2]. Examples of such systems are viscoelastic devices, buckling-restrained braces (BRB) and friction dampers. In spite of several advantages of energy dissipation devices, relatively large residual displacement is the major deficiency in these systems. Moreover, current technologies demonstrate some restrictions including problems related to temperature dependence performance, serviceability and resilience and complications related to installation and substitution.

Application of SMA-based self-centering systems received significant attention from scholars and designers recently. SMAs are unique class of alloys with capability to recover their original shape upon unloading (Superelastic Effect-SE) and heating above a transformation temperature (Shape Memory Effect-SME) [3]. The striking characteristics of SMAs can be attributed to thermal effect or stress-induced phenomenon. Considering its exclusive properties, SMA wire is used as a core recentering component in the SCHD.

Several numerical and experimental studies have shown the workability of SMAs in vibration mitigation of structural systems. Desroches and Delemont [4] have investigated the effectiveness of SMA bars to hinder unseating of the bridge deck from the pier. A modern base isolation system composed of steel-teflon flat sliding bearings was proposed by Jalali et al. [5]; they used SMA truss elements to provide a proper restoring capability. Besides, Cardone et al. [6] conducted an experimental investigation of the Smart Restorable Sliding Base Isolation System (SRSBIS) using superelastic Shape Memory Alloy (SMA) wires, and the outcomes revealed that the SRSBIS can be reliably used in passive control of structures. Dolce et al. [7] evaluated the effectiveness of SMA braces in reinforced concrete structures, results from shaking table test demonstrated that SMA bars can provide favorable self-centering capability. In addition to the mentioned applications, SMAs gained widespread popularity in framed structures. Dolce et al. [8] tested special types of braces using promising properties of SMA during the 'Memory Alloys for New Seismic Isolation and Energy Dissipation Devices' project, the working mechanisms of the device verified the new design concept. Ozbulut and Hurlebaus [9] introduced a recentering variable friction device for vibration limitation of structures subjected to near-field excitations. Simulation results demonstrate that the proposed device has the capability to reduce the peak structural response. Zhu and Zhang [10] investigated the seismic response of a concentrically braced frame (CBF) with reusable hysteretic damping brace made of energy-dissipating SMA wires, results show that the proposed system has a potential to eliminate the residual interstory drift. In another study, Zhu and Zhang [11] suggested a type of bracing element

* Corresponding author.

http://dx.doi.org/10.1016/j.istruc.2015.10.013
2352-0124/

named self-centering friction damping brace for utilization in CBF systems, recentering characteristic of the device is satisfied with stranded superelastic SMA wires while energy dissipation procedure is complemented by means of friction. Yang et al. [12] proposed an innovative hybrid device that combined energy dissipation and recentering components. According to the presented formula of force distribution between the components, the hybrid damper showed recentering capability with maximum energy dissipation capacity. Motahari et al. [13] implemented a damper using different phases of SMA to produce a reasonable behavior which is efficient for both energy dissipation and recentering capabilities. Asgarian and Moradi [14] evaluated the seismic performance of steel frames equipped with SMA braces. The results indicated that SMAs are favorable materials which lead to reduction in residual displacement and peak interstory drift. Jalaeefar and Asgarian [15] developed and tested a hybrid damping device with energy-dissipating and recentering characteristics using steel and SMA bars, respectively. Besides, the optimum proportion of SMA and steel was obtained in various analyses. Ma and Yam [16] examined a self-centering damper with recentering and energy dissipating components group. Their studies show that the controlled structure vibrates around its initial position. Salari and Asgarian [17] investigated seismic performance of steel braced frames using SMA-based hybrid damper. Results proved the efficiency of the device in seismic response mitigation.

McCormick et al. [18] evaluated a novel CBF to compare its seismic performance with traditional systems. They applied rigid bracing members with continuous SMA in whole brace. Krumme et al. [19] have proposed a SMA-based damper for passive control of structures. The success of the proposed damper was revealed through the experiments conducted by Clark et al. [20].

The favorable concept behind the SCHD is the parallel use of the two different sub-components that slightly increases the preliminary building design cost and markedly mitigates the cost related to seismic events. Functional simplicity, moderate encumbrance under installation condition and great durability are the most important features of SCHDs. The main concentration of previous studies was on the reduction of structural responses such as interstory drift. However, similar trend was not observed in time history of acceleration, especially during the earthquake. This response has effectively reduced using the proposed SCHD.

1.1. Shape memory alloys

The dual-phase microstructure of SMAs displays two distinct crystal structures: the austenite phase stable at higher temperatures with body-centered cubic structure, and the martensite phase which is the weaker SMA stable at lower temperatures with parallelogram structure. The presence of stress and temperature changes triggers the transformation between the two crystallographic phases. External stress and temperature have mutual effects on the transformation mechanism. In other words, higher stress leads to higher transition temperatures. There are four critical temperatures that pinpoint the start and final of the straight and reversal transformation. M_s and M_f indicate the martensite start and finish temperatures, respectively. While A_s and A_f denote the austenite start and finish temperatures. Fig. 1 illustrates a stress-strain diagram of SMA under isothermal transformation when $T>A_f$. A considerable strain of 8%-10% will be fully recovered at the end of the applied load [21]. A plump hysteresis loop with zero residual strain will be produced under this unique behavior (SE). A small number of parameters are required to compose the constitutive model which represents the mechanical properties of SMAs. σ_S^{AS} and σ_F^{AS} are starting and final stresses in martensite forward transformation which equal to 525 MPa and 600 MPa, respectively. Similarly, σ_S^{SA} and σ_F^{SA} are martensite to austenite starting and final stresses which equal to 250 MPa and 100 MPa, respectively. E_{SMA} is the elasticity modulus of SMA which equals to 21,500 MPa in austenite and martensite phases [15].

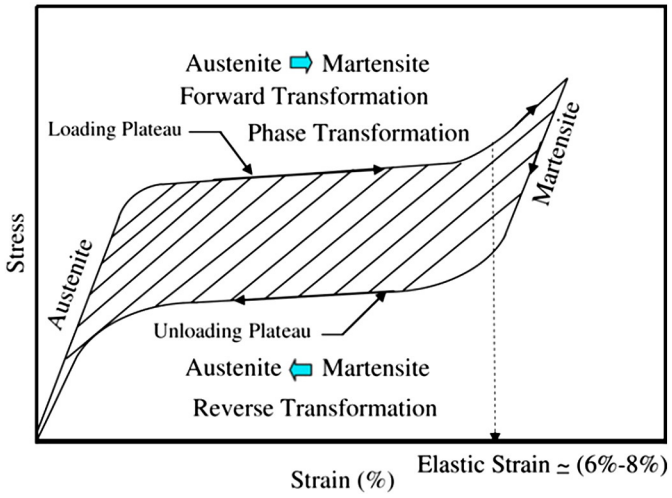

Fig. 1. Stress-strain relationship of superelastic SMA wires [21].

Some different types of SMAs are evaluated based on their mechanical and durability properties. Among them, NiTi is considered as the most popular alloy in vibration control of structures. The main reasons include its extraordinary fatigue and corrosion resistance, preferable superelastic behavior and great durability.

In order to evaluate the effectiveness of SMA wires, cyclic performance of 16 different SCHDs is compared with similar dampers in the absence of SMA wires. Residual displacement and dissipated energy of dampers with different incorporation of SMA are determined to obtain an optimum loop shape. First, a detailed specification of SCHD and its modeling procedure are presented.

2. Description of SCHD mechanism

The schematic of the SCHD for use between the beam and braces is indicated in Fig. 2(a). As can be seen in Fig. 2(b), the device is fabricated of two subcomponents: two pairs of identical transverse SMA wires and a steel pipe. Two plates are installed at both ends for exerting boundary conditions. The benefits of using steel pipe come from its excellent energy dissipation capacity upon yielding and its low cost. Besides, due to being independent from loading rate and surrounding temperature, energy dissipation through steel yielding is a trustworthy method. The hysteretic behavior of SCHD is determined using superposition of flag-shaped hysteresis loop of SMA wires and rectangular curve obtained from yielding of steel pipe. The combined hysteresis loop shows a self-centering behavior accompanied by favorable energy dissipation capability. Owing to high fatigue life of NiTi wires, SCHD can be designed to withstand several intense aftershocks without workability deterioration. For recentering group upon loading, the relative displacement between the two plates will induce tension in one of the two transverse SMA wires, while the wires in another direction simply go slack. Each wire is comprised of several SMA wires with submillimeter diameters to provide the required cross sectional area. Therefore, due to the probability of buckling, compression section of the stress-strain curve is ignored. Furthermore, this movement triggers the energy dissipation process through the deformation of steel pipe. It should be noted that the end plates need to be thick enough to remain elastic under lateral loading.

2.1. Steel and SMA wire modeling

Cyclic loading analyses of SCHDs were carried out using ABAQUS finite element program [22]. The steel used in this study was tested by Maleki and Bagheri to evaluate the shear pipe damper performance, and yield stress of the material is assumed to be equal to 250 MPa [23].

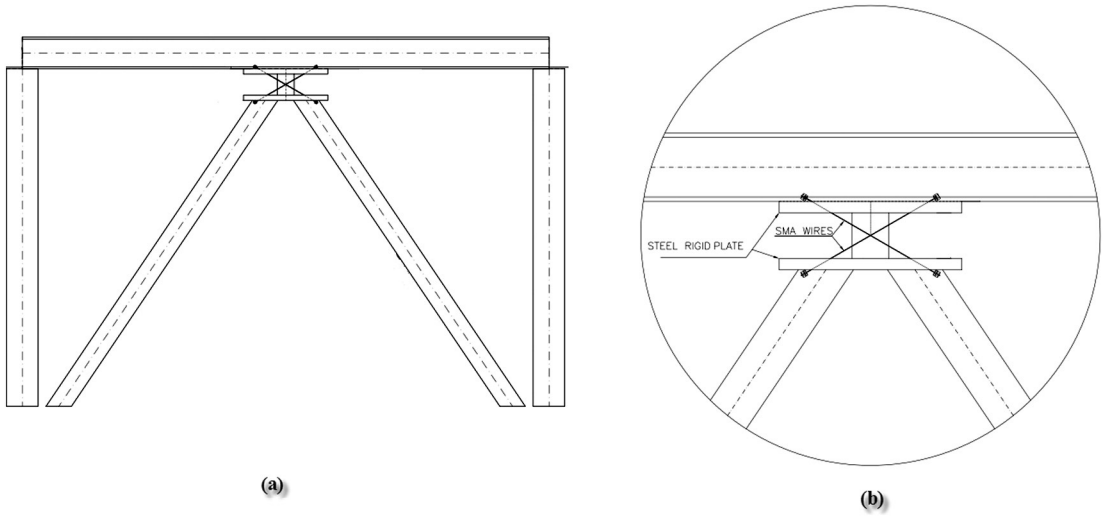

Fig. 2. Hybrid damper. (a) Placement in frame structure. (b) Mechanical configuration of SCHD.

Due to the lack of SMA in ABAQUS material library, the stress-strain relationship is exactly applied in the model through user-defined material. In each step, the finite element program presents the strain variations to FORTRAN and the program provides the corresponding stress. The tests conducted by Jalaeefar and Asgarian showed the NiTi behavior when it was subjected to tension [15]. The experiments were carried out to ascertain the mechanical properties of 8 mm diameter NiTi bars. Although SMAs show recentering property in the strain range of 8–10%, a conservative value of 6% is applied to avoid the second stiffening occurrence. This phenomenon can result in serious damage to adjacent members. Using this concept, the over design of connections can be prevented and the fatigue life of SMAs can rise into myriad load cycles.

Cyclic behavior of the SMA wire should be evaluated to assure that the outcome is in accordance with real condition. In order to assess the results, SMA wire is loaded to the maximum allowable strain of 6%. Fig. 3 illustrates a comparison between the experimental and numerical simulations for SMA bar. As can be seen, in spite of trivial inconsistency in residual strain, there is a good agreement between the two results.

The boundary conditions are modeled by limiting all nodes of the bottom plate from moving and rotating in all directions which means that it is fixed. The nodes located at the left edge of the top plate are pushed in the form of displacement in the X-direction. Fig. 4 depicts the mentioned boundary conditions and the exerted load.

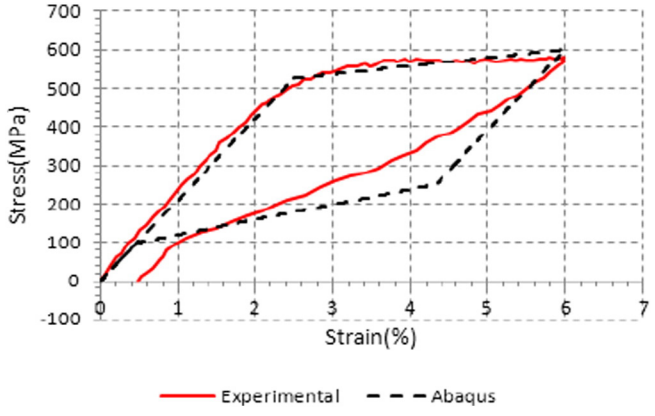

Fig. 3. Verification of F.E model with experimental results.

3. Parametric study

Adjustable design parameters including design load, incorporation percentage of SMA, height of the damper and inclination angle of SMA wires are the promising features of SCHDs compared to other SMA-based dampers. Incorporation percentage of SMA is the fraction of design load which is assumed to be sustained by SMA wires. Parametric study is

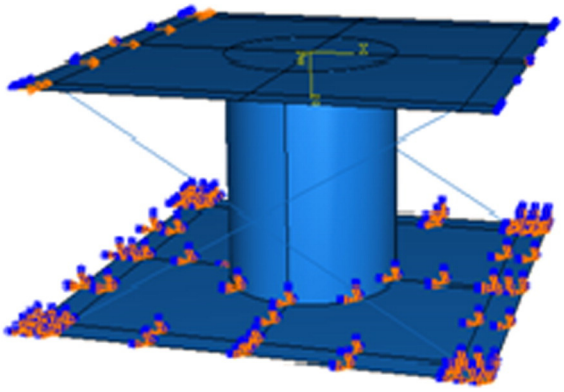

Fig. 4. Boundary conditions and applied load.

Table 1
Properties of designed dampers for parametric study.

P (KN)	L (m)	Incorporation percentage of SMA (%)	r (m)	t (m)	θ	A_{SMA} (m^2)	Sample ID
1500	0.2	80%	0.08	0.0065	30°	0.001319	A
					45°	0.001616	B
		40%	0.08	0.0195	30°	0.00066	C
					45°	0.000808	D
	0.3	80%	0.11	0.0047	30°	0.001319	E
					45°	0.001616	F
		40%	0.11	0.0141	30°	0.00066	G
					45°	0.000808	H
2000	0.2	80%	0.08	0.0087	30°	0.001759	I
					45°	0.002155	J
		40%	0.08	0.026	30°	0.00088	K
					45°	0.001077	L
	0.3	80%	0.11	0.0063	30°	0.001759	M
					45°	0.002155	N
		40%	0.11	0.0189	30°	0.00088	O
					45°	0.001077	P

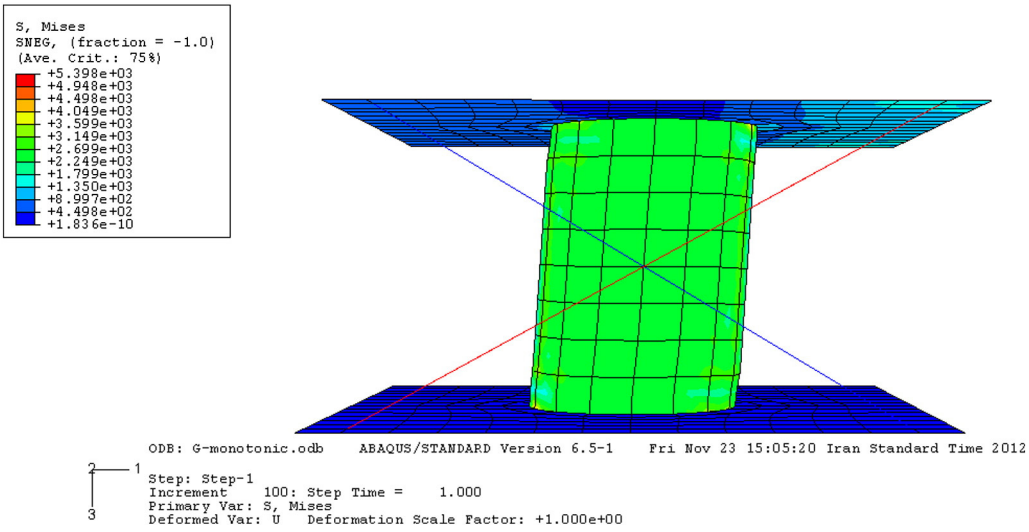

Fig. 5. Deformation of components under cyclic loading.

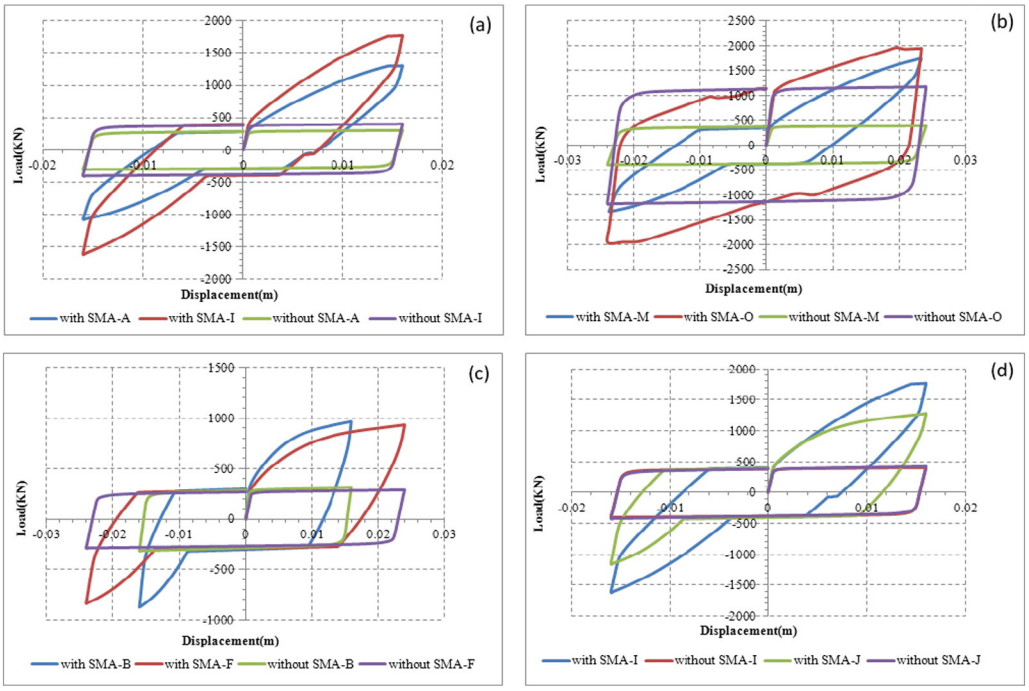

Fig. 6. Effect of design parameters on SCHD hysteresis loops. (a) Design load. (b) Incorporation percentage of SMA. (c) Damper height. (d) Wire inclination angle.

conducted to determine the effect of these parameters on seismic performance of SCHDs. Therefore, behavior of 16 instances of SCHDs has been investigated under cyclic loading to evaluate their efficiency. $V_{SMA} = 2F_{SMA}\cos\theta$ is applied to design the recentering component of the SCHD. F_{SMA} is the axial load induced in the wires, and it is used to determine the cross-sectional area of wires and θ is the wire inclination angle. Table 1 presents properties of samples named as A-P. P, L, r and t represent the design load, length, radius and thickness of the pipe, respectively.

3.1. Static cyclic analysis

A nonlinear static analysis with reversal load is conducted to study the behavior of SCHD. The deformed shape at maximum displacement of the top plate is illustrated in Fig. 5. As noted before, four damper parameters are assessed in this parametric study. Each comparison contains two selective cases from Table 1.

3.1.1. Effect of design load

This section examines the effect of design load on damper performance. Fig. 6(a) shows the hysteresis loops of SCHDs subjected to displacement loading. Two cases that include A and I with identical incorporation of SMA, pipe length and wire inclination angle are

Table 2
Equivalent viscous damping ratio.

Sample ID	Energy loss (KN m)	Strain energy (KN m)	ξ_{eq}
A	21.33	10.42	16.2%
B	23.25	7.71	24%
F	33.43	11.18	23.7%
I	29.09	14.14	16.3%
J	30.94	10.23	24%
M	38.08	20.25	15%
O	106.04	19.16	44%

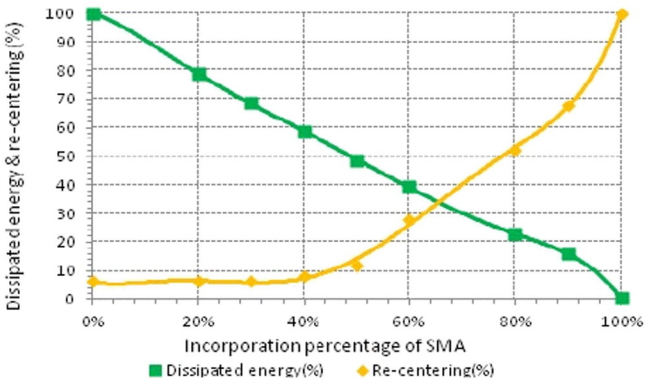

Fig. 7. Determination of optimum incorporation percentage of SMA.

selected to determine the load level at which the performance of SCHD is more desirable. As can be seen in Fig. 6(a), SCHD which is designed to sustain higher load level has larger pipe thickness. Therefore, it reveals better energy absorption capability and higher stiffness. In spite of this conclusion, both cases have almost the same recentering capability of 50%. Consequently, an increment in design load cannot modify the recovered displacement. For a better understanding of the effect of SMA wires on SCHD recentering performance, similar analysis was conducted on the identical dampers in the absence of SMA wires. The outcome shows that the dampers equipped with SMA wires are perfectly capable of reducing the residual displacements.

3.1.2. Effect of incorporation percentage of SMA

A parametric study on the effect of incorporation percentage of SMA was carried out and results are illustrated in this section. Two cases including M and O were considered for this investigation. M and O have different incorporation percentages of SMA, accounting for 80% and 40%, respectively. Taking a closer look at the juxtaposed load-displacement curves in Fig. 6(b) indicates that the SCHD with lower incorporation percentage of SMA is more powerful for energy dissipation as a result of higher pipe strength, whereas it has trivial ability to recover the displacement.

As another important result, displacement reduction of 58% can be attributed to case M. It should be noted that asymmetry in the hysteresis loop for case M is due to dissimilar buckling of steel pipe under tension and compression. A comparison similar to former section is conducted to highlight the effect of SMA wires. Comparison between these dampers emphasizes that energy absorption capability of thicker steel pipe is nearly three times as high as damper with thinner wall pipe.

3.1.3. Effect of damper height

Damper height is another adjustable parameter which is discussed in this section. As shown in Fig. 6(c), by comparing cases with two different heights, it is found that this parameter could not considerably impress the displacement reduction. Greater ductility of case F results in

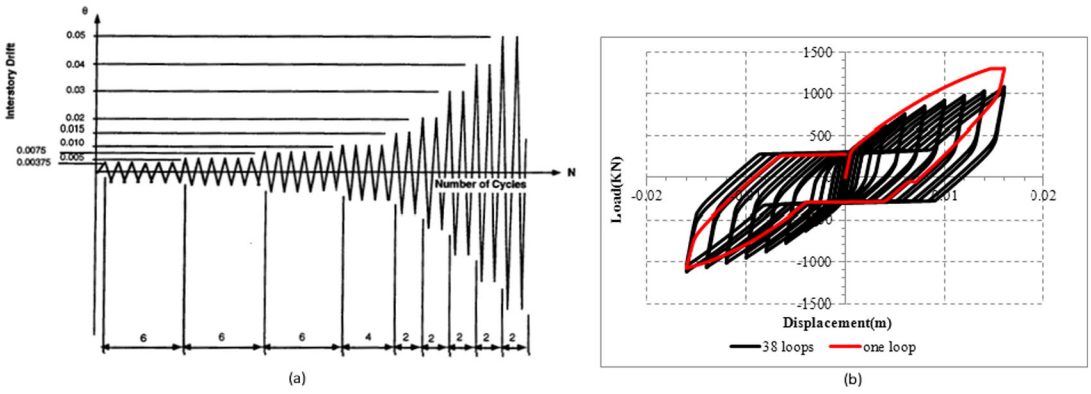

Fig. 8. Effect of several loading cycles. (a) Loading protocol of SAC. (b) Comparison between results.

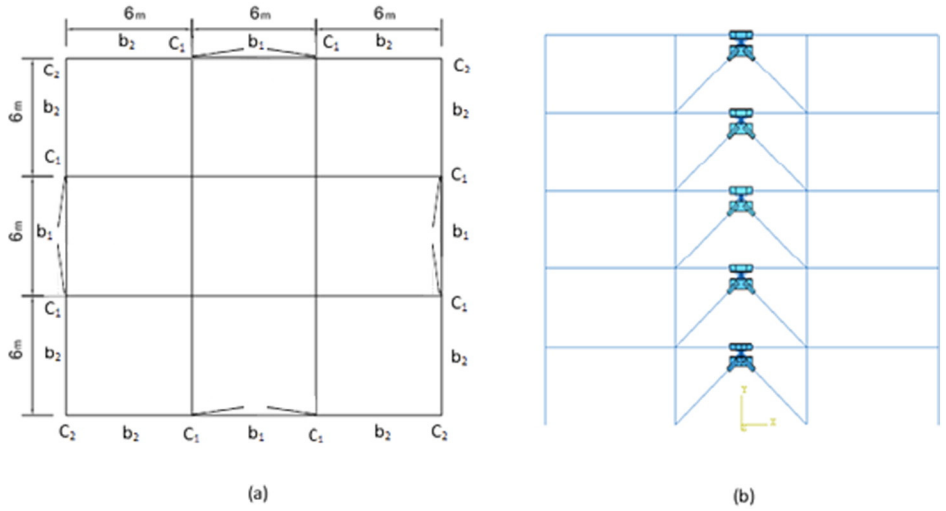

Fig. 9. Schematic of modelled structure. (a) Plan. (b) Elevation.

Table 3
Designed members of the controlled structure.

Story	Middle columns	Edge columns	Middle beams	Edge beams	Braces
1	*TUBO*300×300×30	*TUBO*150×150×12	*HEB*300	*HEB*200	*TUBO*200×200×20
2	*TUBO*300×300×30	*TUBO*150×150×12	*HEB*300	*HEB*200	*TUBO*200×200×20
3	*TUBO*200×200×20	*TUBO*150×150×10	*HEB*300	*HEB*200	*TUBO*200×200×20
4	*TUBO*200×200×20	*TUBO*150×150×10	*HEB*300	*HEB*200	*TUBO*200×200×14
5	*TUBO*200×200×20	*TUBO*150×150×10	*HEB*300	*HEB*200	*TUBO*200×200×14

more energy absorption capability. Due to the buckling effect which is observed in thin-walled pipes, the design load of dampers cannot be achieved. Moreover, results extracted from the cases without SMA wires clearly evidence the favorable effect of damper height in energy absorption capability.

3.1.4. Effect of SMA wire inclination angle

This section presents the results of changing SMA wire inclination angle. Fig. 6(d) depicts two cases with different wire slopes: case I has lower wire inclination angle compared to case J. The results indicate that by applying larger cross sectional area for each wire the energy absorption capability is slightly improved, whereas there is an approximately considerable permanent displacement. Besides, it can be concluded that two SCHDs have relatively similar loop area while case I has greater strength. Because of all mentioned reasons, SCHD with lower wire slope has more desirable performance under cyclic loading.

As a result of having identical pipes, elimination of SMA wires cannot change SCHD cyclic behavior. On the other hand, dampers without SMA wires have lower energy absorption and larger permanent displacement in comparison with SCHDs.

3.2. Energy consideration

For proving the efficiency of the proposed device, equivalent viscous damping ratio is calculated. As can be seen in Eq. (1), results are obtained based on the ratio between the dissipated energy in each cycle (A_h) and strain energy (A_e). Details corresponding to the calculations can be found in Table 2. Results indicate that sample "O" has the best efficiency in enhancing the equivalent damping of SCHD.

$$\xi_{eq} = \frac{A_h}{4\pi A_e} \tag{1}$$

4. Optimum incorporation percentage of SMA

There are two superior properties in SCHD performance including residual drift mitigation and energy absorption improvement. As described above, incorporation percentage of SMA is the most effective parameter in enhancing SCHD performance. So, an ideal performance can be obtained by changing the load contribution of SMA. Dissipated energy and recentering for samples with various incorporation percentages of SMA are evaluated and results are depicted in Fig. 7. It should be noted that the size of design load, pipe height and inclination angle of wires are constant in each point of the curves. In order to express the absorbed energy as a percent, all energy amounts are normalized to their maximum values. As concluded from the parametric study, the amount of dissipated energy decreases by increasing the incorporation percentage of SMA. Conversely, the percentage of recovered displacement has a direct relationship with incorporation percentage of SMA. Furthermore, in smaller incorporation percentages there is not a considerable increment in recentering values while the amount of the absorbed energy sustains a significant decrement. In other words, below the incorporation percentage of 40%, role of SMA wires in displacement reduction is negligible. So, utilization of expensive SMA wires would not be economical.

In order to satisfy the objective of energy dissipation, it would be more reasonable to dedicate smaller incorporation percentage to SMA wires. On the other hand, higher values are used to prevent the permanent displacement. This should be limited to the value which results in a reasonable thickness for the steel pipe. The intersection of the two curves is the optimum point where both objective properties are at the greatest amounts simultaneously. This occurs in SMA incorporation percentage of 63%. It is interesting to note that the definition of the optimum point depends on the performance level which SCHD is designed for.

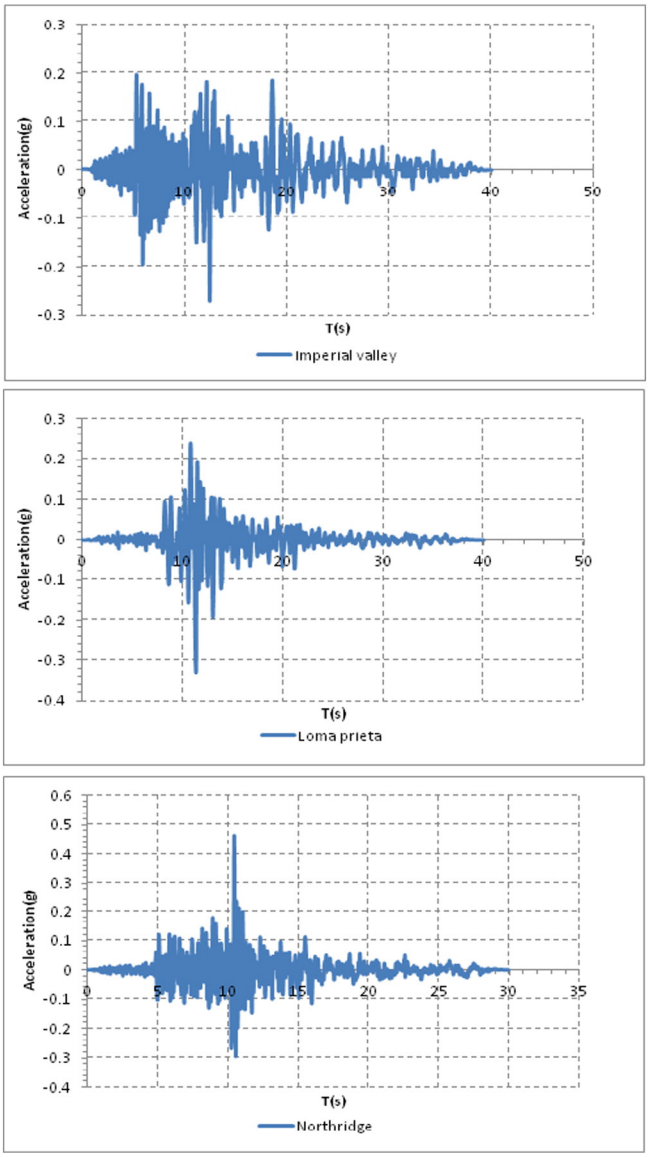

Fig. 10. Ground motion records data.

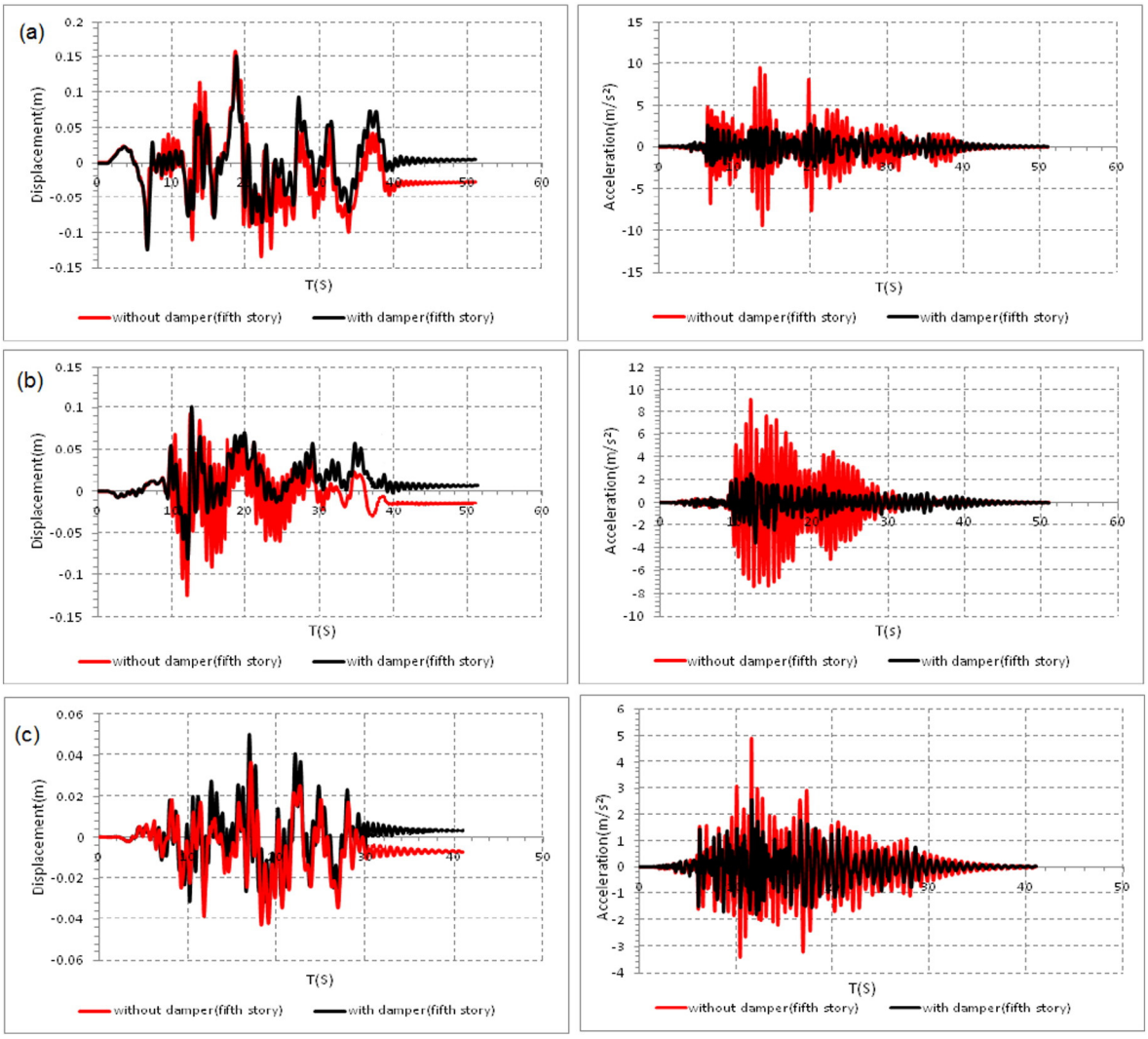

Fig. 11. Roof displacement and acceleration time histories. (a) Imperial Valley, (b) Loma Prieta, and (c) Northridge.

5. Effect of several loading cycles

In order to assess the response of SCHD subjected to several loading cycles, one of the defined cases is selected and exposed to SAC loading protocol which is a joint venture of Structural Engineering Association of California (SEAOC), Applied Technology Council (ATC) and California Universities for Research in Earthquake Engineering (CUREE) [12]. According to the SAC protocol, the loading path consists of several cycles with increasing amplitude which pushes the sample to 3% of its length. Fig. 8(a) represents the SAC loading protocol. Loading results reveal that the sample which sustained 38 loops of displacement loading can better indicate the effect of buckling. As can be seen in Fig. 8(b), a considerable difference between two curves shows that results of loading under several cycles are more reliable due to proximity to reality.

6. Nonlinear time history analysis

In this section, results of nonlinear time history analysis of a 5-story building are presented to evaluate the effectiveness of SCHD in permanent drift mitigation. The results are compared with seismic response of ordinary braced frame. The building is square in plan and consisted of 3 spans of 6 m in each direction and the story height of 3.2 m.

As can be seen in Fig. 9, middle bays in both directions are eccentrically braced. Hybrid damper is placed between the beam and chevron braces. It should be noted that the occurrence of out-plane buckling can be avoided by selection of pipe section as energy dissipation component with its high lateral torsional buckling strength. In order to reach the shear performance of the link, pipe length is assumed to be 0.3 m. The calculated radius of the pipe is 0.1 m, this is properly based on AISC criterion in which $L<1.6\sqrt{3}r$. The main structural members will remain in elastic range as a result of capacity design rule. Building member properties used in numerical study are given in Table 3. Seismic response of this special frame is compared with ordinary concentric braced frame.

As previously mentioned, the device was designed based on capacity design rule. This methodology serves to confine ductility demands to members which have specific requirements to ensure their ductile behavior. Other members of the EBF must be designed based on the shear and flexural yield capacities of the vertical link in order to have elastic behavior before the vertical link reaches the yield capacity. Therefore, the adjacent members of a link are designed to remain elastic. SMA wires are responsible for reducing the relative displacement between the top and bottom plates. In other words, yielding of structural fuse stimulates the potential re-centering capacity of the frame.

It should be mentioned that different values of incorporation percentage of SMA are assigned to each story level. This selection is based on the restrictions of pipe design. The pipe wall will be thin as a result of high incorporation percentage of SMA; this will lead to intense

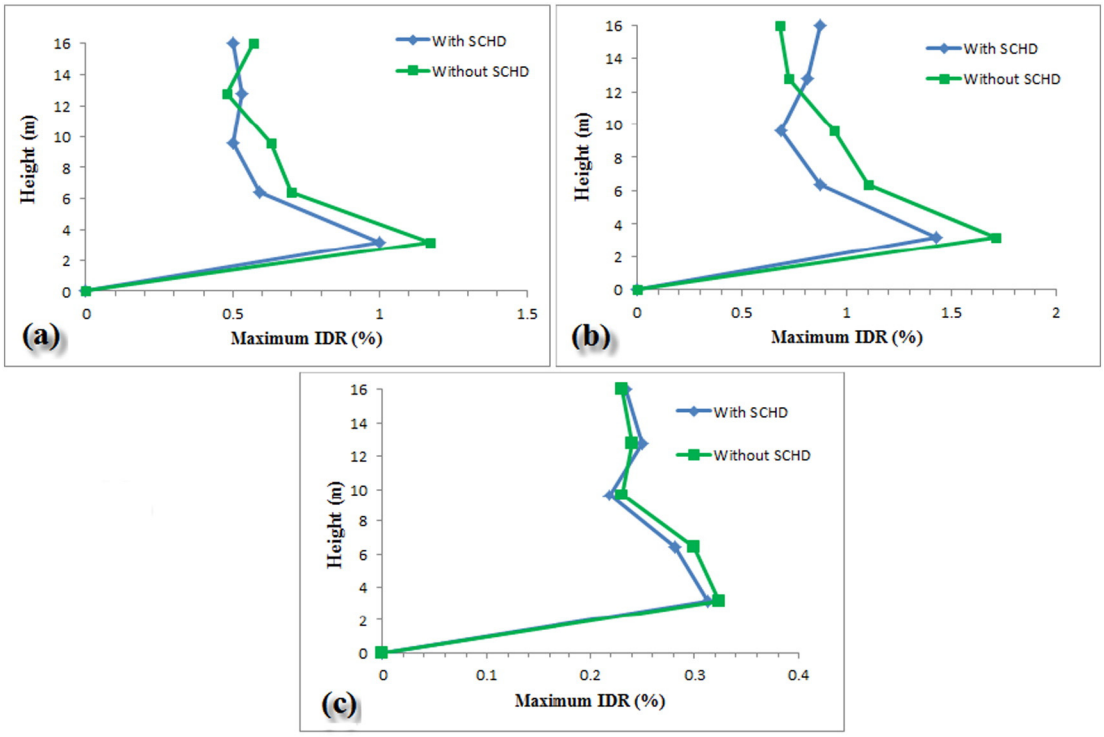

Fig. 12. Profiles of maximum interstory drift ratio. (a) Imperial Valley, (b) Loma Prieta, and (c) Northridge.

possibility of buckling. So, the incorporation percentage of 50%, 50% and 40% is chosen for the first, second and third story, respectively. In other words, the fourth and fifth stories have no SMA wires. The length of the pipe is considered to be 0.3 m for all stories. In addition, the wire inclination angle is 30° for the first three stories. Cross-sectional areas of SMA wires are 2200 mm^2, 2053 mm^2 and 1408 mm^2 for the first, second and third story, respectively.

Nonlinear dynamic analyses are conducted through ABAQUS finite element program. The Imperial Valley, Loma Prieta and Northridge earthquakes are applied to assess the efficiency of the structure. The peak ground accelerations of the records are 0.27 g, 0.329 g and 0.465 g, respectively. In order to evaluate the effect of SMA wires on permanent roof displacement, free vibration is considered at the end of the earthquake. Fig. 10 shows the ground motion records.

Fig. 11 shows time histories of roof displacement and acceleration for both controlled and uncontrolled frames under three excitations. The first natural period of the structure is 0.78 s, whereas the corresponding value for ordinary braced frame is 0.64 s. As can be seen, hybrid damper is very effective in suppressing the roof permanent displacement, accounting for approximately 92% under Imperial Valley earthquake. This is due to the self-centering potential of the proposed damper which yields a double flag-shaped hysteresis. This unique property allows the SCHD to revert back to its initial condition after unloading. The difference between results originates from different frequency contents of earthquakes.

As shown in Fig. 11, the hybrid damper is very effective in suppressing the displacements during the earthquakes. Maximum displacement reduction occurs during the Loma Prieta earthquake, accounting for 97%. As can be seen, during the Northridge earthquake displacements cannot be perfectly reduced. The main reason is that the strains in SMA wires negligibly enter into their second slope. So, this earthquake is not a strong excitation for strain stimulation in the wires.

In addition, the value of acceleration decreases during the applied earthquake; maximum acceleration responses decreased by 73% under the Loma Prieta earthquake. The main reason is the role of steel pipe in energy absorption capability. As a result, it can be claimed that the steel pipe is very effective in shear force absorption.

The maximum Interstory Drift Ratio (IDR) over the height of the structure is illustrated in Fig. 12. As can be seen, SCHD has its ideal workability under the Loma Prieta earthquake; maximum IDR reduction of 37% occurs in the third floor of the structure equipped with SCHD. A fairly similar distribution can be observed for IDR under the Imperial Valley earthquake, amounting to 26%. On the other hand, lack of SMA wires can be observed in IDR reduction for the fourth and fifth floors where larger values can be seen for the controlled structure. It can be concluded that SMA wires with their recentering properties are effective elements in reduction of IDR values.

Under the Northridge earthquake, the SCHD is not very effective in suppressing the maximum IDR. As mentioned before, this excitation cannot induce enough strain in SMA wires. So, a negligible reduction is observed for this record.

7. Summary and conclusions

The research investigated the cyclic behavior of a self-centering hybrid damper which is comprised of energy dissipating and recentering components. Hysteretic behavior of SMA which resulted from numerical modeling was in good agreement with experimental results. Furthermore, parametric study was performed to evaluate the effect of design parameters on the SCHD characteristics. Results indicated that increase in wire slope unfavorably affects the flag-shaped hysteresis loop of SCHD.

It should be pointed out that a methodology for optimal design of SCHDs could be one of critical improvements in this type of structural control. An optimization process was performed to obtain an incorporation percentage of SMA at which both promising properties of SCHD have ideal values. Then, the effect of cycle numbers on hysteresis loops of SCHD was investigated. The results indicated that loading under several cycles is reliable due to better representation of buckling.

Embedment of hybrid damper between the beam and bracing system will concentrate the fundamental damages within these special devices. So, the main structural system is intended to have little or no damage. The outcomes of nonlinear time history analysis showed that

the hybrid damper can reduce the permanent displacement, peak interstory drifts and acceleration of the seismically excited structure.

Results of the investigation emphasized that performance of the steel component as an axial member could better improve the recentering property of the SCHD. Thus, further researches are essential to investigate the behavior of SCHDs with both components under axial loading. In addition, it seems necessary to confirm the numerical results experimentally.

Acknowledgments

Financial support from the Iranian National Science Foundation (INSF), grant no. INSF 91004065 is gratefully acknowledged.

References

[1] Constantinou MC, Soong TT, Dargush GF. Passive energy dissipation systems for structural design and retrofit. Buffalo (NY): Research Foundation of the State University of New York and Multidisciplinary Center for Earthquake Engineering Research; 1998.
[2] Karavasilis T, Kerawala S, Hale E. Hysteretic model for steel energy dissipation devices and evaluation of a minimal-damage seismic design approach for steel buildings. J Constr Steel Res 2012;70:358–67.
[3] Duerig TW, Melton KN, Stoeckel D, Wayman CM. Engineering aspects of shape memory alloys. London: Butterworth-Heinemann Ltd; 1990.
[4] Desroches R, Delemont M. Seismic retrofit of simply supported bridges using shape memory alloys. Eng Struct 2002;24:325–32.
[5] Jalali A, Cardone D, Narjabadifam P. Smart restorable sliding base isolation system. Bull Earthq Eng 2011;9(2):657–73.
[6] Cardone D, Narjabadifam P, Nigro D. Shaking table tests of the smart restorable sliding base isolation system (SRSBIS). J Earthq Eng 2011;15(8):1157–77.
[7] Dolce M, Cardone D, Ponzo FC, Valente C. Shaking table tests on reinforced concrete frames without and with passive control systems. Earthq Eng Struct Dyn 2005;34:1687–717.
[8] Dolce M, Cardone D, Marnetto R. Implementation and testing of passive control devices based on shape-memory alloys. Earthq Eng Struct Dyn 2000;29:945–68.
[9] Ozbulut OE, Hurlebaus S. Recentering variable friction device for vibration control of structures subjected to near-field earthquakes. Mech Syst Signal Process 2011;25:2849–62.
[10] Zhu S, Zhang Y. Seismic behaviour of self-centring braced frame buildings with reusable hysteretic damping brace. Earthq Eng Struct Dyn 2007;36:1329–46.
[11] Zhu S, Zhang Y. Seismic analysis of concentrically braced frame systems with self-centering friction damping braces. J Struct Eng 2008;134(1):121–31.
[12] Yang W, DesRoches R, Leon RT. Design and analysis of braced frames with shape memory alloy and energy-absorbing hybrid devices. Eng Struct 2010;32:498–507.
[13] Motahari SA, Ghassemieh M, Abolmaali SA. Implementation of shape memory alloy dampers for passive control of structures subjected to seismic excitations. J Constr Steel Res 2007;63:1570–9.
[14] Asgarian B, Moradi S. Seismic response of steel braced frames with shape memory alloy braces. J Constr Steel Res 2011;67:65–74.
[15] Jalaeefar A, Asgarian B. A simple hybrid damping device with energy dissipating and recentering characteristics for special structures. Struct Design Tall Spec Build 2012;23(7):483–92.
[16] Ma H, Yam M. Modelling of a self-centring damper and its application in structural control. J Constr Steel Res 2011;67:656–66.
[17] Salari N, Asgarian B. Seismic response of steel braced frames equipped with shape memory alloy-based hybrid devices. Struct Eng Mech 2015;53(5):1031–49.
[18] McCormick J, DesRoches R, Fugazza D, Auricchio F. Seismic assessment of concentrically braced steel frames with shape memory alloy braces. J Struct Eng 2007;133(6):862–70.
[19] Krumme R, Hayes J, Sweeney S. Structural damping with shape-memory alloys: one class of devices. Proceeding SPIE, 2445. ; 1995. p. 225–40.
[20] Clark PW, Aikn ID, Kelly JM, Higashino M, Krumme RC. Experimental and analytical studies of shape memory alloy dampers for structural control. Proceeding SPIE1995, 2445. 1995. p. 51–241.
[21] Sharabash AM, Andrawes BO. Application of shape memory alloy dampers in the seismic control of cable-stayed bridges. Eng Struct 2009;31:607–16.
[22] ABAQUS Version 6.5. Hibbitt, Karlsson& Sorensen, Inc., Pawtucket, RI.
[23] Maleki S, Bagheri S. Pipe damper, part I: experimental and analytical study. J Constr Steel Res 2010;66:1088–95.